JOURNAL OF MATERIALS SCIENCE 4 (1969) 518–525

Some Observations on the Deformation Characteristics of Bulk Polycrystalline Zirconium Hydrides

Part 1 *The Deformation and Fracture of Hydrides Based on the δ-Phase*

K. G. BARRACLOUGH, C. J. BEEVERS
Department of Physical Metallurgy and Science of Materials, The University, Edgbaston, Birmingham 15, UK

Received 20 December 1968

The deformation behaviour of bulk polycrystalline zirconium hydrides in the composition range $ZrH_{1.27}$ to $ZrH_{1.66}$ has been investigated by compressive loading at temperatures between room temperature and ~ 500° C. Single-phase δ-zirconium hydride is brittle below ~ 100° C. Analyses of slip traces on δ specimens deformed at temperatures between ~ 100 and ~ 250° C have shown that the glide planes are {111} types. The deformation characteristics of δ and (δ + γ) alloys at temperatures between ~ 100 and ~ 500° C are consistent with the hydrogen vacancies in the δ-phase providing significant lattice friction to the movement of dislocations in the zirconium lattice of the hydride structure. The room temperature fracture stress of (δ + γ) alloys increases with the volume fraction of the γ-phase and this can be related to the resistance offered by γ platelets to the propagation of cleavage cracks in the δ matrix. In a (δ + γ + α) alloy the resistance to crack propagation at room temperature is further increased by the soft α-zirconium phase.

1. Introduction

Three zirconium hydrides, γ, δ and ε are known to form in the zirconium-hydrogen system. At room temperature the single-phase δ hydride is formed at compositions between ~ $ZrH_{1.60}$ and ~ $ZrH_{1.67}$. The δ-phase is based on the CaF_2 structure so that the hydrogen atoms occupy some of the tetrahedral interstices of a fcc zirconium lattice [1]. The γ-phase is a metastable product of the δ-phase, and it has been shown that, in slow-cooled alloys, a decrease in hydrogen content from ~ $ZrH_{1.60}$ to ~ $ZrH_{1.30}$ results in an increase in the volume fraction of the γ-phase from 0 to ~ 44% at room temperature [2, 3]. Neutron diffraction measurements have shown that in the γ-phase the hydrogen atoms occupy ordered tetrahedral sites in a fct zirconium lattice, which has c/a > 1 [1]. At hydrogen contents greater than ~ $ZrH_{1.67}$ the δ-phase transforms to the ε-phase which has a fct structure with c/a < 1 [2].

There have been several investigations of the mechanical behaviour of transition metal hydrides contained in their respective metal matrices [4-6]. The hydride precipitates are extremely brittle below ~ 150° C; above this temperature they appear to exhibit some degree of plastic deformation. However, the deformation behaviour of bulk transition metal hydrides has received little attention. Beck and Mueller [7] studied the tensile properties of zirconium hydrides within the composition range $ZrH_{0.7}$ to $ZrH_{1.9}$ and within the temperature range ~ 20 to ~ 600° C. Macroscopic plastic deformation was not observed in the single-phase δ and ε hydrides over the complete temperature range investigated.

The present paper is concerned with the

deformation and fracture behaviour of bulk zirconium hydrides in the composition range $ZrH_{1.27}$ to $ZrH_{1.66}$. At room temperature, the hydride of composition $ZrH_{1.27}$ has a δ matrix with second phase of γ- and α-zirconium; the hydrides in the composition range $ZrH_{1.47}$ to $ZrH_{1.57}$ have a δ matrix with second-phase γ precipitates, and the $ZrH_{1.66}$ hydride is single-phase δ.

2. Experimental

The zirconium used as the base material for these experiments was fabricated from arc-melted, iodide zirconium bar into 3.175 mm plate. The zirconium contained less than 1000 ppm by weight of impurities, the principle of these being H, Hf, Ni, Fe and O. Tensile specimens with parallel-sided gauge lengths of $\sim$ 12.7 mm and gauge widths of 3.175 mm were machined from the zirconium plate which had been rolled to 0.76 mm sheet. Rods, $\sim$ 50 mm $\times$ 3.175 mm $\times$ 3.175 mm, were also prepared from the zirconium plate. The tensile specimens and rods were ground flat and chemically polished in a solution containing 45 parts H_2O, 45 parts HCl and 10 parts HF by volume.

The zirconium specimens were converted to zirconium hydrides of controlled composition by a technique involving the reaction of zirconium with hydrogen at 800° C [2]. The reaction rates between the zirconium and hydrogen were controlled so that homogeneous, crack free specimens were obtained on slow cooling to room temperature. This method was used successfully to produce tensile specimens of $ZrH_{1.66}$ and rods of $ZrH_{1.66}$, $ZrH_{1.57}$, $ZrH_{1.52}$, $ZrH_{1.47}$ and $ZrH_{1.27}$. However, zirconium hydrides in the composition range $ZrH_{1.60}$ to $ZrH_{1.65}$ always exhibited some degree of cracking after preparation. The hydrided tensile specimens exhibited extensive warping which could not be eliminated by metallographic grinding; the hydrided zirconium rods were not extensively warped and a metallographic polishing treatment was successfully used to remove the rumpled surfaces. Compression specimens with height-to-base ratios of $\sim$ 3 : 1 were cut from the hydrided rods. Individual specimens were subsequently mechanically polished to a 0.25 μm diamond finish and lightly etched in a solution containing by volume, 45 parts H_2O, 45 parts HNO_3 and 10 parts HF. Metallographic observations of all specimens revealed grain sizes in the range 0.38 to 0.27 mm.

Specimens were deformed in a hard beam tensometer at a strain rate of 3.3×10^{-4} sec^{-1}. Tests at 20° C were performed in air and a silicone oil bath was used to achieve test temperatures between 20 and 200° C. For test temperatures between 200 and 500° C an electrical resistance furnace was used and tests were carried out in an atmosphere of high purity argon maintained at a pressure of 760 torr.

3. Results

3.1. Tensile Deformation and Fracture of Single-Phase $\delta ZrH_{1.66}$

Fracture always preceded measurable plastic deformation in tensile specimens which were tested between 22 and 500° C. The stress at fracture was in the range 4.9 kg/mm^2 to 7.0 kg/mm^2 and did not vary significantly with test temperature. However, since fracture did not always take place within the gauge lengths, owing to non-axial loading of the warped specimens, these results should only be considered qualitatively.

3.2. Compressive Deformation and Fracture of Single-Phase $\delta ZrH_{1.66}$

The nominal stress/strain curves of $ZrH_{1.66}$ specimens tested at various temperatures between 22 and 453°C are shown in fig. 1. Many of these tests were interrupted to allow metallographic examination of the specimens. Consequently, the total strains in fig. 1 are only those to fracture where indicated. Below $\sim$ 100° C the specimens were completely brittle and macroscopic deformation could not be detected from either examination of polished specimen surfaces or deviations from proportionality of the stress/strain curves. Small plastic strains (up to $\sim$ 3%), could be accommodated in the specimens at temperatures between 100 and 120° C prior to transgranular fracture. Metallographic examination of the polished surfaces of these fractured specimens revealed cracks and planar slip lines. Above 120° C the intensity of slip marking increased (fig. 2), and wavy slip lines were a predominant feature of specimens tested above 250° C.

Microbeam X-ray and two-face stereographic analysis techniques were used to determine the active slip planes in the δ-zirconium hydrides. From specimens tested at 109° C an analysis showed that the operative slip planes were of the {1 1 1} type. This observation was supported by several single-face analyses from specimens

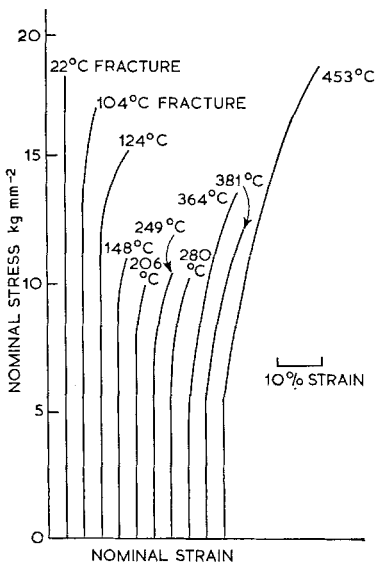

Figure 1 Nominal stress/strain curves for the compressive deformation of $ZrH_{1.66}$ in the temperature range 22 to 453° C.

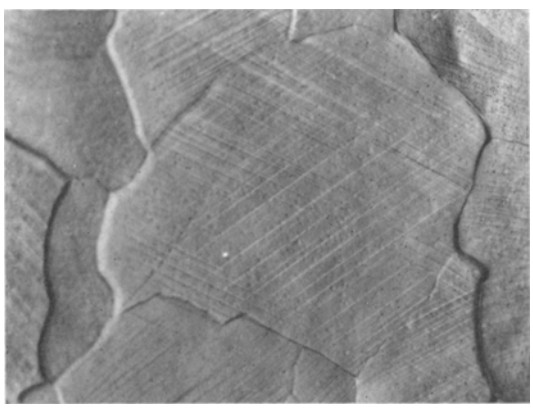

Figure 2 Surface slip lines on a specimen of $ZrH_{1.66}$ after 2% plastic strain at 148° C (× 90).

tested at 100, 104 and 109° C. From specimens given 2% plastic strain at 124, 148, 166 and 206° C, two-face analyses showed that, as in the lower temperature range, the operative slip planes were also of the {1 1 1} type. At temperatures above 250° C the slip traces were extremely wavy and could not be analysed to give unambiguous results.

3.3. Compressive Deformation of ($\delta + \gamma$) and ($\delta + \gamma + \alpha$) Hydrides

Hydrides of composition $ZrH_{1.57}$, $ZrH_{1.52}$ and $ZrH_{1.47}$ ($\delta + \gamma$) and $ZrH_{1.27}$ ($\delta + \gamma + \alpha$) were tested at temperatures between 22 and 500° C. The limit of proportionality of these specimens and that of $\delta ZrH_{1.66}$ is plotted as a function of test temperature in fig. 3. In the temperature range 22 to 100° C the limit of proportionality increased considerably with decreasing hydrogen content.

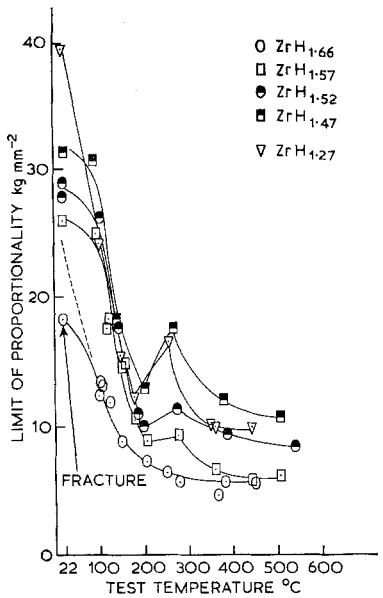

Figure 3 Temperature dependence of the limit of proportionality of δ, ($\delta + \gamma$) and ($\delta + \gamma + \alpha$) hydrides.

From 100 to 200° C the limit of proportionality of the ($\delta + \gamma$) and ($\delta + \gamma + \alpha$) hydrides decreased rapidly and, over most of the temperature range, was virtually independent of hydrogen content. Surfaces of lightly deformed specimens revealed planar slip lines in the δ matrix (fig. 4); internal sections of heavily deformed specimens contained distorted γ platelets (fig. 5). The $ZrH_{1.27}$ specimens also deformed by slip in the δ grains, but the deformation was inhomogeneous (fig. 6).

Unlike the single phase $\delta ZrH_{1.66}$ specimens the ($\delta + \gamma$) hydrides exhibited marked peaks in their limit of proportionality/temperature curves at $\sim$ 270° C (fig. 3). The difference between the limit of proportionality at 200 and 270° C increased as the hydrogen content decreased. Examination of sectioned specimens of $ZrH_{1.52}$ and $ZrH_{1.57}$ tested above 280° C showed that the γ platelets tended to be much finer than those in the "as-grown" hydrides. Furthermore, they did not show the distortions which were a feature of these alloys tested below 200° C (fig. 5). These

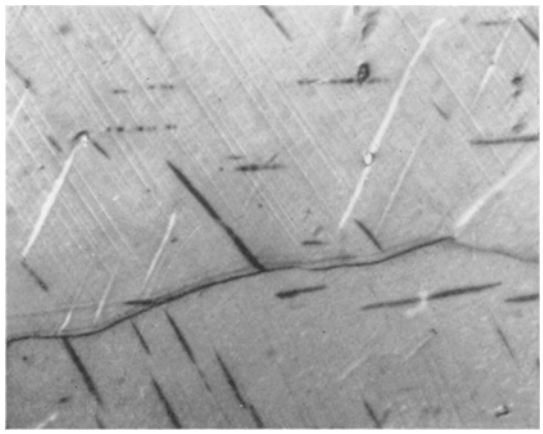

Figure 4 Planar slip lines in the δ matrix of a $ZrH_{1.57}$ specimen after 2.5% plastic strain at 117° C. Polarised light (× 350).

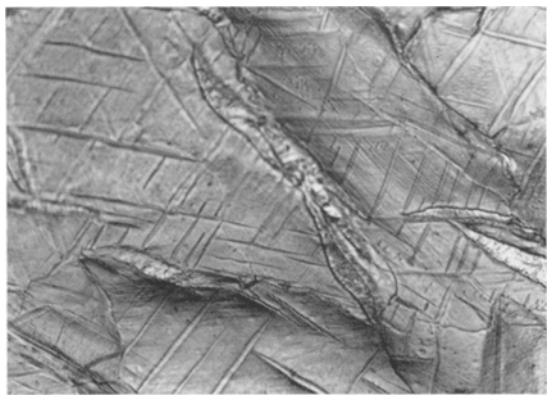

Figure 6 The surface of a $ZrH_{1.27}$ specimen after ~6% plastic strain at 178° C showing the γ platelets within the δ grains, the α-zirconium phase at the δ grain-boundaries and localised slip bands (× 177).

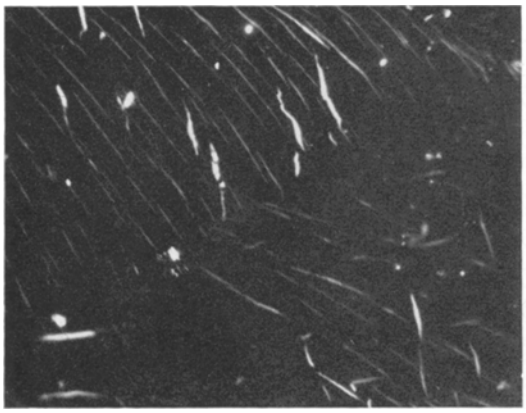

Figure 5 Distorted γ platelets in a $ZrH_{1.57}$ specimen sectioned after 26% plastic strain at 204° C. Polarised light (× 245).

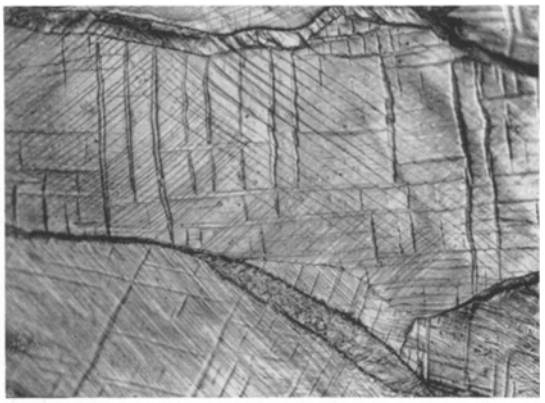

Figure 7 Large distorted γ platelets on a $ZrH_{1.27}$ specimen after 11% strain at 360° C (× 111).

results show that the γ-phase was probably taken into solution above ~ 200° C and subsequently re-precipitated on cooling to room temperature. The $ZrH_{1.27}$ ($\delta + \gamma + \alpha$) alloys did not show the changes in mechanical behaviour above 200° C which might have been expected simply on the basis of hydrogen content (fig. 3). Examination of a $ZrH_{1.27}$ hydride after deformation at 360° C showed the presence of large distorted γ platelets (fig. 7), which indicates that the γ-phase was not completely taken into solution at the test temperature.

In the temperature range 400 to 500° C the room temperature ($\delta + \gamma$) alloys are considered to be single-phase δ, and it can be seen from fig. 3 that the limit of proportionality increases with decreasing hydrogen content.

3.4. Fracture of ($\delta + \gamma$) and ($\delta + \gamma + \alpha$) Hydrides at Room Temperature

Unlike the room temperature stress/strain curves of $\delta ZrH_{1.66}$ specimens, those of the ($\delta + \gamma$) hydrides exhibited small but positive deviations from proportionality prior to complete specimen failure. Examination of the specimens after fracture did not reveal extensive slip traces. However, surface cracks which had apparently been either arrested or deflected by the γ platelets (fig. 8) were evident. Two series of interrupted tests were performed to examine the formation of these surface cracks on $ZrH_{1.47}$ and $ZrH_{1.52}$ specimens. Surface cracks were first observed at

19.3 kg/mm² and 19.0 kg/mm² in the $ZrH_{1.47}$ (fig. 9a) and $ZrH_{1.52}$ specimens respectively. Subsequent increases in stress resulted in the nucleation of new cracks and growth of the existing ones. Comparison of fig. 9a with 9b shows the growth of an individual crack on $ZrH_{1.47}$ after increasing the stress level from 19.3 kg/mm² to 26.4 kg/mm². The $ZrH_{1.47}$ specimen had a nominal stress/strain curve which deviated from proportionality at 31.7 kg/mm²; fracture occurred at 34.2 kg/mm². In the stress interval between 31.7 kg/mm² and 34.2 kg/mm² significant crack broadening occurred.

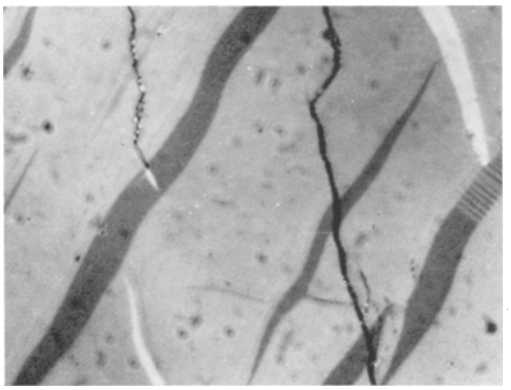

Figure 8 The surface of a $ZrH_{1.52}$ specimen after 0.5% strain at room temperature, showing a crack arrested in a γ platelet. Polarised light (× 690).

A stress level of 45.8 kg/mm² was achieved in a test on the $ZrH_{1.27}$ specimen at room temperature without total fracture taking place. This test was limited in stress range by the capacity of the testing arrangement. Examination of this $ZrH_{1.27}$ specimen which had achieved $\sim 1\%$ strain revealed the presence of surface cracks, as in the $(\delta + \gamma)$ alloys. However, the surface cracks appeared to be primarily arrested at the grain-boundary α-phase (fig. 10).

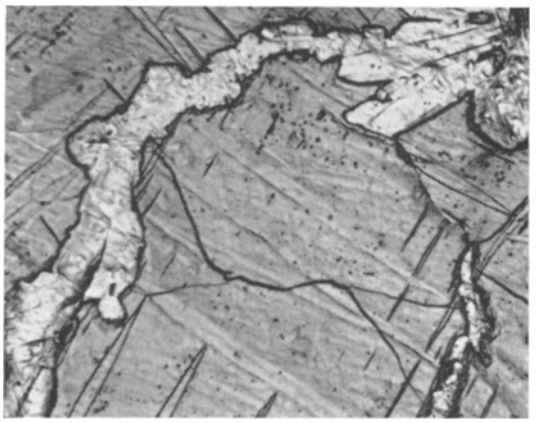

Figure 10 A branched crack arrested at the grain-boundary α-zirconium phase in a $ZrH_{1.27}$ specimen after 1% strain at room temperature. Polarised light (× 300).

The deformation and fracture behaviour of the hydrides at room temperature are summarised in fig. 11, in which the stresses for (A) crack formation, (B) deviations from proportionality of the stress/strain curve and (C) fracture are plotted as a function of hydrogen content. The stress for crack formation in the δ hydride was not measured from interrupted tests and it is assumed that initial crack formation was the

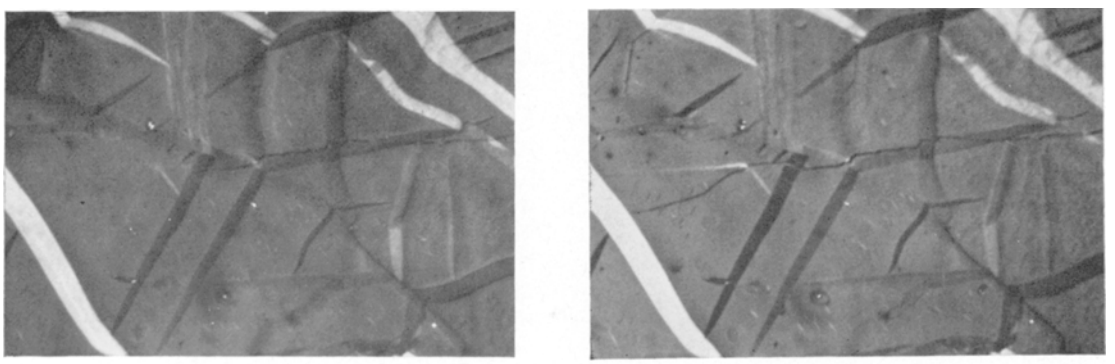

(a) (b)

Figure 9 Surface crack on a $ZrH_{1.47}$ specimen loaded at room temperature to, (a) 19.3 kg/mm² and, (b) 26.4 kg/mm². Polarised light (× 480).

critical event which led directly to complete fracture.

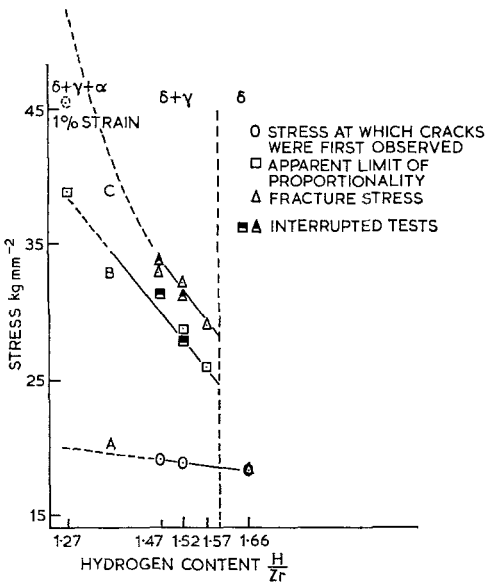

Figure 11 The fracture and deformation characteristics of δ, (δ + γ) and (δ + γ + α) hydrides at room temperature.

4. Discussion

4.1. Deformation of δ-Zirconium Hydrides

Plastic deformation in $\delta ZrH_{1.66}$ specimens was associated with slip on {111} planes; {100} and {110} slip traces were not observed over the temperature range examined. The Burgers vectors of the glide dislocations in the δ-phase have not been determined but it is expected that these are a/2 ⟨110⟩ types, since an a/2 ⟨110⟩ translation returns both the zirconium and hydrogen atoms to their equilibrium positions. Indeed, a/2 ⟨110⟩ dislocations have been observed in CaF_2 [8], UO_2 [9] and ThO_2 [10] which possess the same fluorite crystal structure as δ-zirconium hydride. However, since in an ionic compound the operative glide planes are influenced by the electrical interactions between the ions, the predominant slip planes of CaF_2, UO_2 and ThO_2 are {100} types [8-10]; {111} and {110} slip planes are only observed in these compounds when, at elevated temperatures, the ionic bonding is relaxed. The occurrence of slip on {111} planes in δ-zirconium hydride is, therefore, indicative of considerable metallic bonding which appears to dominate the ionic component in determining the operative glide planes. The predominance of metallic bonding in zirconium hydride is also evident from its thermodynamic and electrical properties [11].

Assuming that the slip systems of the δ-phase are {111} ⟨110⟩ types, the extreme room temperature brittleness could possibly be a result of the hydrogen lattice exerting considerable restrictions on the movement of zirconium lattice glide dislocations. Whilst the mechanical properties of the δ-phase over its non-stoichiometric composition range were not investigated at room temperature, a decrease in microhardness from $ZrH_{1.60}$ (240 VDH) to $ZrH_{1.66}$ (200 VDH) has been observed [12]. Furthermore, in the temperature range 400 to 500° C, where the original (δ + γ) hydrides are believed to be single-phase δ, the limit of proportionality decreases with an increase in hydrogen content. Both these observations support the contention that the hydrogen vacancies act as the primary source of lattice friction to the movement of dislocations. This behaviour may be contrasted with that of TiC [13] which also has a {111} ⟨110⟩ type slip system. However, a decrease in the carbon content reduces the yield stress, since the primary resistance to dislocation movement arises from the strong covalent bonding between the titanium and carbon atoms.

One feature of the stress/strain curves in fig. 1 is the relatively high work-hardening rate which was maintained over the temperature range examined. This may be an inherent property of the δ lattice but, on the other hand, it could arise from the rather high dislocation densities (10^9 lines/cm^2), which have been observed in as-grown transition metal hydrides [14].

The limit of proportionality of the $ZrH_{1.66}$ specimens decreased rapidly above 100° C (fig. 3). This may possibly be ascribed to the partial collapse of the hydrogen lattice due to increased mobility of the hydrogen atoms. However, the hydrogen vacancies still maintain their effectiveness in restricting dislocation movement even at 400 to 500° C, as evidenced by the limits of proportionality of the δ-phase alloys in this temperature range.

4.2. Deformation of (δ + γ) and (δ + γ + α) Hydrides

The limits of proportionality of the $ZrH_{1.57}$, $ZrH_{1.52}$ and $ZrH_{1.47}$ alloys decreased rapidly from 100 to 200° C and were virtually independent of hydrogen content over this temperature range (fig. 3). These observations are consistent with the (δ + γ) alloys having a δ matrix of the

same composition ($\sim ZrH_{1.59}$), and the limit of proportionality being primarily controlled by the deformation characteristics of the δ matrix. It should be noted that, at a given temperature, the limit of proportionality of the $(\delta + \gamma)$ alloys was always greater than that of the single phase δ, as would be expected on the basis of the previous discussion concerning the role of hydrogen vacancies. The γ platelets were distorted during deformation (fig. 5) and, whilst they would provide barriers to dislocation movement, they are not considered on the basis of their morphology to have a significant influence on the yield characteristics between 100 and 200° C.

The discontinuities in the curves of fig. 3 above 200° C are believed to be associated with a phase change in the $(\delta + \gamma)$ alloys. Sidhu *et al* [1] have reported that a transformation from $(\delta + \gamma)$ to $(\delta + \alpha)$ occurs at $\sim 250°$ C, and Beck [3] has reported fast reaction kinetics for the dissolution of the γ-phase. It is suggested that the increase in the limits of proportionality of the $(\delta + \gamma)$ alloys above 200° C is a result of an increased hydrogen vacancy concentration in the δ matrix produced by the dissolution of the γ-phase. It should be noted that the increase in the limit of proportionality between 200 and 270° C is greater for the alloys with lower hydrogen content (fig. 3), as would be expected if the hydrogen vacancy content in the δ matrix was effective in controlling yield characteristics. The dissolution of the γ-phase is also consistent with the room temperature metallographic observations of $(\delta + \gamma)$ alloys which exhibited fine undistorted γ platelets after deformation above 200° C.

The $ZrH_{1.27}$ $(\delta + \gamma + \alpha)$ alloy appears to be anomalous in that the limit of proportionality curve above $\sim 200°$ C lies between those for the $ZrH_{1.52}$ and $ZrH_{1.47}$ $(\delta + \gamma)$ alloys. However, even after deformation at 360° C, large distorted γ platelets were observed (fig. 7), and this indicates that not all the γ-phase was taken into solution. In such a situation the δ matrix would have a composition dependent upon the reaction kinetics for the three-phase alloy but could be expected to be below $ZrH_{1.59}$. Indeed, the equilibrium phases and their compositions for $ZrH_{1.27}$ as a function of temperature are not known, but qualitatively a partial dissolution of the γ-phase, as indicated experimentally, is consistent with the overall mechanical properties.

4.3. Fracture of the Zirconium Hydrides

The $ZrH_{1.66}$ δ-phase specimens tested in tension between room temperature and 500° C were extremely brittle and these observations are in general agreement with those of Beck and Mueller [7].

The existence of available $\{111\}\langle 110\rangle$ type slip systems woud appear to satisfy the von Mises criterion [15] for polycrystalline ductility and it must be concluded that the restriction of some of these slip systems by the lattice friction effects of the hydrogen vacancies is responsible for the brittleness of the δ-phase when tested in compression below $\sim 100°$ C.

The formation of cracks in the δ-phase appears to occur at approximately the same stress level for both $\delta ZrH_{1.66}$ and $ZrH_{1.59}$ (fig. 11). Libowitz and Pack [16] have reported $\{111\}$ cleavage planes in single crystals of cerium dihydride. If, as seems reasonable, δ-zirconium hydride also exhibited such a cleavage plane, then with $\{111\}$ slip planes the mechanism proposed by Stroh [17], whereby crack nucleation occurs by low angle boundary separation, would appear to be the most appropriate. Although no direct observations of crack nuclei were made, low angle boundaries were a common feature of the as-grown hydrides [2].

The influence of the volume fraction of the γ-phase on the room temperature fracture stress of $(\delta + \gamma)$ alloys is shown in fig. 12. Now, metallographic observations of the $(\delta + \gamma)$ alloys revealed that with an increase in volume fraction of γ-phase the size and also the interspacing of the platelets increased. If the primary role of the γ platelets was to act as crack nucleation centres through dislocation pile-up activity, then the fracture stress might be expected to decrease with an increase in the particle interspacing, i.e. with increasing volume fraction of γ-phase, a conclusion which is not supported by the results in fig. 12. The results in fig. 11 show that cracks were formed at stress levels well below those for final fracture; this indicates that the marked increase in fracture stress may be associated with the restriction of crack growth by the γ platelets. The observations presented in figs. 8 and 9a show that the γ platelets can arrest or deflect cleavage cracks in the δ matrix. The γ platelets have a $\{100\}$ habit plane in the δ matrix [2]. Thus, if the cleavage planes in the δ- and γ-phases are the same, probably of the $\{111\}$ type, then the cracks must change their directions of propagation to pass through the γ platelets. The γ platelets also exhibit a twinned structure which, by retwinning, could possibly offer further

resistance to crack propagation (fig. 8). In general therefore, the results would appear to support the idea that the primary role of the γ platelets was to inhibit crack propagation rather than to influence crack nucleation processes. The results on the ($\delta + \gamma + \alpha$) alloy are rather limited but, as might be expected, the soft α-zirconium-phase is more efficient than the γ-phase in restricting the growth of cleavage cracks in the δ matrix (figs. 10 and 11).

The results in fig. 11, considered in relation to the preceding discussion, imply that in the region A-B, crack nucleation and propagation occur, and that the apparent limit of proportionality (curve B) is primarily a consequence of specimen shape change through crack propagation and broadening rather than plastic deformation. This process of crack propagation and broadening continues through region B-C to fracture at curve C.

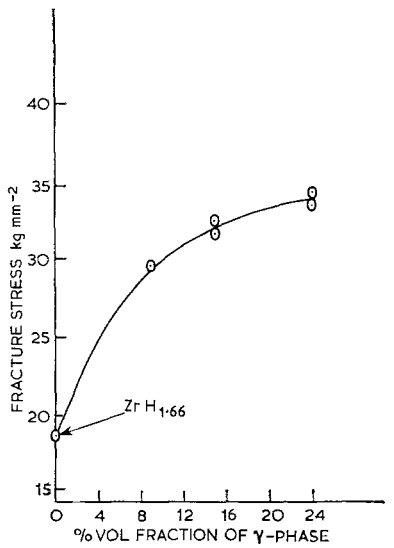

Figure 12 Influence of volume fraction of second-phase γ platelets on the room temperature fracture stress of ($\delta + \gamma$) alloys.

5. Conclusions

(i) Single-phase δ-zirconium hydride exhibits no measurable or observable macroscopic plastic deformation when tested in compression below $\sim 100°$ C.

(ii) Analyses of slip traces observed on single-phase δ hydrides deformed between ~ 100 and $\sim 250°$ C have shown that the operative glide planes are of the {1 1 1} type.

(iii) The deformation characteristics of δ- and ($\delta + \gamma$)-zirconium hydrides between ~ 100 and $\sim 500°$ C are consistent with hydrogen lattice vacancies providing a significant frictional resistance to dislocation movement in the δ-phase.

(iv) The fracture stress of ($\delta + \gamma$) alloys at room temperature increases with the volume fraction of γ-phase, and this can be related to the resistance offered by γ platelets to the propagation of cleavage cracks in the δ matrix.

Acknowledgement

The authors wish to thank Professor G. V. Raynor for the provision of laboratory facilities. This work was sponsored by the Metallurgy Division, AERE Harwell, and the authors gratefully acknowledge financial assistance and the provision of a studentship for K G B.

References

1. S. S. SIDHU, N. S. SATYA MURTHY, F. P. CAMPOS, and D. D. ZAUBERIS, *Adv. Chem. Ser.* **39** (1963) 87.
2. K. G. BARRACLOUGH and C. J. BEEVERS, to be published.
3. R. L. BECK, *Trans. ASM* **55** (1962) 542.
4. C. J. BEEVERS, M. R. WARREN, and D. V. EDMONDS, *J. Less Comm. Met.* **14** (1968) 387.
5. G. W. PARRY and W. EVANS, *Electrochem. Tech.* **4** (1966) 225.
6. M. R. WARREN and C. J. BEEVERS, *Met. Sci. J.* **1** (1967) 173.
7. R. L. BECK and W. M. MUELLER, "Nuclear Metallurgy", Vol. VII (Met. Soc. AIME, 1960) p. 63.
8. C. ROY, Ph.D. Thesis (Imperial College, London, 1962).
9. K. H. G. ASHBEE, Reported by B. Beagley and J. W. Edington, *Brit. J. Appl. Phys.* **14** (1963) 609.
10. J. W. EDINGTON and M. J. KLEIN, *J. Appl. Phys.* **37** (1966) 3906.
11. T. R. P. GIBB, *Prog. Inorg. Chem.* **3** (1962) 315.
12. K. G. BARRACLOUGH, Ph.D. Thesis (University of Birmingham, 1968).
13. G. E. HOLLOX and R. E. SMALLMAN, *J. Appl. Phys.* **37** (1966) 818.
14. P. E. IRVING, M.Sc. Thesis (University of Birmingham, 1968).
15. R. VON MISES, *Z. angew Math. Mech.* **8** (1928) 161.
16. G. G. LIBOWITZ and J. G. PACK, "Proc. Int. Conf. on Crystal Growth", edited by H. S. Peiser (Pergamon Press, Oxford & New York, 1966) p. 129.
17. A. N. STROH, *Phil. Mag.* **3** (1958) 597.